VII International Conference on Computational Methods for Coupled Problems in Science and Engineering
COUPLED PROBLEMS 2017
M. Papadrakakis, E. Oñate and B. Schrefler (Eds)

HOMOGENIZATION OF THE FLUID-SATURATED PIEZOELECTRIC POROUS METAMATERIALS

Eduard Rohan*, Vladimír Lukeš* and Robert Cimrman†

* European Centre of Excellence, NTIS – New Technologies for Information Society Faculty of Applied Sciences, University of West Bohemia, Univerzitní 8, 30614 Pilsen, Czech Republic
rohan@kme.zcu.cz

† New Technologies Research Centre, University of West Bohemia, Univerzitní 8, 30614 Pilsen, Czech Republic cimrman3@ntc.zcu.cz

Key words: Multiscale modelling, Piezoelectric material, Porous media, Homogenization, Sensitivity analysis, Nonlinear problems

Abstract. The paper is devoted to the homogenization approach in modelling of periodic porous media constituted by piezoelectric porous skeleton with pores saturated by viscous fluid. The representative volume element contains the piezoelectric solid part (the matrix) and the fluid saturated pores (the channels). Both the matrix and the channels form connected subdomains. The mathematical model describing the material behaviour at the microscopic scale involves the quasi-static equilibrium equation governing the solid piezoelectric skeleton, the Stokes model of the viscous fluid flow in the channels and the coupling interface conditions on the transmission interface. The macroscopic model is derived using the unfolding method of homogenization. The effective material coefficients are computed using characteristic responses of the porous microstructure. The constitutive law for the upscaled piezo-poroelastic material involves a coefficient coupling the electric field and the pore pressure. A numerical example illustrates different responses of the porous medium subject to the drained and undrained loadings

1 INTRODUCTION

The piezoelectric effects which couple the mechanical deformation and the electrical field have been extensively used in the design of transducers and sensors. The piezoelectric materials have found wast applications in electronics, mechatronics, and micro-system technology. Smart structures based on these materials allow for intelligent self-monitoring and self-control capabilities. Nowadays the piezoelectric sensor-actuator systems can be distributed continuously, being attached to the surface of other structural parts. Such an arrangement can be used *e.g.* in the aerospace industry to control vibrations, or acoustic radiation of thin flexible structures. In the context of porous piezoelectric materials, the

acoustic wave propagation has been subject of several works [10]. In [4] we suggested to exploit the piezoelectric effect in the design of a new type of bio-materials which should assist in bone healing and regeneration. Such possible application for piezoelectric materials in biomedical engineering is motivated by the electrochemical processes in biological tissues, being coupled tightly with periodic mechanical loading. In [7], the shape sensitivity formulae were derived for a class of 2D microstructures comprising one piezoelectric and one arbitrary elastic material, whereby the shape of the interface between the two materials was parameterized. The numerical tests have shown how a suitable geometry of the interface can amplify some of the homogenized coefficients. Sensitivity of the effective medium properties to the microsrtucture properties were also reported in [9].

This paper is focused on the derivation of the effective material coefficients of the fluid-saturated porous media with the piezoelectric skeleton. Although this topic was treated recently in [3], where a special type of piezoelectric anisotropic composite materials was studied using numerical and analytical methods and the porosity influence was examined, we pursue another homogenization approach which was reported in [6]. Assuming a quasistatic loading, such that inertia effects can be neglected, by a decomposed homogenization of the fluid-structure interaction problem we obtain a macroscopic model of the upscaled medium. Here we present only the resulting equations governing the local problems for computing the characteristic responses which are used to evaluate all the homogenized coefficients involved in the constitutive law. A numerical example is included to demonstrate the influence of the pore fluid on the overall response of the upscaled porous piezoelectric medium.

Notations We employ standard bold-face notations for tensors and vectors, alternatively the Einstein summation convention is used. The Lebesgue spaces of 2nd-power integrable functions on a domain D is denoted by $L^2(D)$, the Sobolev space $\boldsymbol{W}^{1,2}(D)$ of the square integrable vector-valued functions on D including the 1st order generalized derivative, is abbreviated by $\mathbf{H}^1(D)$. Further, $H^1_\#(Y_m)$ and $\mathbf{H}^1_\#(Y_m)$ are the Sobolev spaces of scalar and vector-valued Y-periodic functions (the subscript #), respectively, with vanishing mean in Y_m.

2 HOMOGENIZED MODEL OF POROUS PIEZOELECTRIC MATERIAL

The poroelastic medium occupies an open bounded domain $\Omega \subset \mathbb{R}^3$ whereby the following decomposition of Ω into the matrix and channel parts is considered: $\Omega = \Omega^\varepsilon_m \cup \Omega^\varepsilon_c \cup \Gamma^\varepsilon$, $\Omega^\varepsilon_m \cap \Omega^\varepsilon_c = \emptyset$, where $\Gamma^\varepsilon = \overline{\Omega^\varepsilon_m} \cap \overline{\Omega^\varepsilon_c}$ is the interface. By $\partial_{\rm ext}\Omega^\varepsilon_m = \partial\Omega^\varepsilon_m \setminus \Gamma^\varepsilon$ and $\partial_{\rm ext}\Omega^\varepsilon_c = \partial\Omega^\varepsilon_c \setminus \Gamma^\varepsilon$ we denote the exterior boundaries of Ω^ε_m and Ω^ε_c, respectively. Both Ω^ε_m and Ω^ε_c are connected domains generated by the representative periodic cell $Y = \Pi_{i=1}^3]0, \bar{y}_i[\subset \mathbb{R}^3$ which splits into the solid part occupying domain Y_m and the complementary channel part Y_c, thus

$$Y = Y_m \cup Y_c \cup \Gamma_Y \,, \quad Y_c = Y \setminus Y_m \,, \quad \Gamma_Y = \overline{Y_m} \cap \overline{Y_c} \,. \tag{1}$$

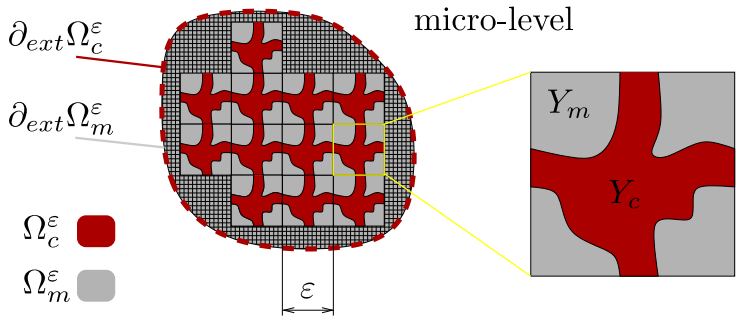

Figure 1: Porous periodic structure in domain Ω is generated using the reference cell Y.

For a given scale, $\ell_i = \varepsilon \bar{y}_i$ is the characteristic size (associated with the i-th coordinate direction, whereby also $\varepsilon \approx \ell_i/L$ for a given macroscopic characteristic length. Below we describe two separate problems which can be upscaled independently, if the inertia effects are neglected:

- steady states of the porous piezoelectric solid saturated by static fluid,
- the Stokes flow in the pores of the undeformed configuration.

2.1 Porous piezoelectric solid saturated by static fluid

We consider the static problem of a deformed piezo-elastic porous structure saturated by a fluid under a constant pressure, whereby the pores are assumed to be connected. In the piezoelectric solid, the Cauchy stress tensor $\boldsymbol{\sigma}^\varepsilon$ and the electric displacement $\vec{D}^\varepsilon$ depend on the strain tensor $\boldsymbol{e}(\boldsymbol{u}^\varepsilon) = (\nabla \boldsymbol{u}^\varepsilon + (\nabla \boldsymbol{u}^\varepsilon)^T)/2$ defined in terms of displacement field $\boldsymbol{u}^\varepsilon = (u_i^\varepsilon)$, and the electric field $\boldsymbol{E}(\varphi^\varepsilon) = \nabla \varphi^\varepsilon$ defined in terms of the electric potential φ^ε, where we adhere to the sign convention employed in [4],

$$\begin{aligned} \sigma_{ij}^\varepsilon(\boldsymbol{u}^\varepsilon, \varphi^\varepsilon) &= A_{ijkl}^\varepsilon e_{kl}^\varepsilon(\boldsymbol{u}^\varepsilon) - g_{kij}^\varepsilon \partial_k \varphi^\varepsilon \ , \\ D_k^\varepsilon(\boldsymbol{u}^\varepsilon, \varphi^\varepsilon) &= g_{kij}^\varepsilon e_{ij}^\varepsilon(\boldsymbol{u}^\varepsilon) + d_{kl}^\varepsilon \partial_l \varphi^\varepsilon \ . \end{aligned} \tag{2}$$

Above, $\mathbb{A}^\varepsilon = (A_{ijkl}^\varepsilon)$ is the elasticity fourth-order symmetric positive definite tensor of the solid, *i.e.* $A_{ijkl} = A_{klij} = A_{jilk}$, the deformation is coupled with the electric field through the 3rd order tensor $\boldsymbol{g}^\varepsilon = (g_{kij}^\varepsilon)$, $g_{kij}^\varepsilon = g_{kji}^\varepsilon$ and $\boldsymbol{d} = (d_{kl})$ is the permitivity tensor.

The state of the solid skeleton is governed by the following boundary value problem involving $\boldsymbol{u}^\varepsilon, \varphi^\varepsilon$ and the static fluid pressure p^ε:

- equilibrium of the stress and electric displacements,

$$\begin{aligned} -\nabla \cdot \boldsymbol{\sigma}^\varepsilon(\boldsymbol{u}^\varepsilon, \varphi^\varepsilon) &= \boldsymbol{f}^\varepsilon \ , \quad \text{in } \Omega_m^\varepsilon \ , \\ -\nabla \cdot \vec{D}^\varepsilon(\boldsymbol{u}^\varepsilon, \varphi^\varepsilon) &= q_E^\varepsilon \ , \quad \text{in } \Omega_m^\varepsilon \ , \end{aligned} \tag{3}$$

  where $\boldsymbol{f}^\varepsilon$ is the volume-force and q_E^ε is the volume electric charge;

- mass conservation (change of fluid and solid volume due to fluid injection $-J^\varepsilon$)

$$\int_{\partial\Omega_c^\varepsilon} \boldsymbol{u}^\varepsilon \cdot \boldsymbol{n}^{[c]} \,\mathrm{dS}_x + \gamma p^\varepsilon |\Omega_c^\varepsilon| = -J^\varepsilon \,, \tag{4}$$

  where γ is the fluid compressibility;

- boundary and interface conditions,

$$\begin{aligned} \boldsymbol{n}^{[m]} \cdot \boldsymbol{\sigma}^\varepsilon(\boldsymbol{u}^\varepsilon, \varphi^\varepsilon) &= \boldsymbol{h}^\varepsilon \,, \quad \text{on } \partial_{\mathrm{ext}}\Omega_m^\varepsilon \,, \\ \boldsymbol{n}^{[m]} \cdot \boldsymbol{\sigma}^\varepsilon(\boldsymbol{u}^\varepsilon, \varphi^\varepsilon) &= -p^\varepsilon \boldsymbol{n}^{[m]} \,, \quad \text{on } \Gamma^\varepsilon \,, \\ \boldsymbol{n}^{[m]} \cdot \vec{D}^\varepsilon(\boldsymbol{u}^\varepsilon, \varphi^\varepsilon) &= \varrho_E^\varepsilon \,, \quad \text{on } \partial_{\mathrm{ext}}\Omega_m^\varepsilon \,, \\ \boldsymbol{n}^{[m]} \cdot \vec{D}^\varepsilon(\boldsymbol{u}^\varepsilon, \varphi^\varepsilon) &= 0 \,, \quad \text{on } \Gamma^\varepsilon \,, \end{aligned} \tag{5}$$

  where $\boldsymbol{n}^{[m]}$ is the outer unit normal vector of the boundary Ω_m^ε, $\boldsymbol{h}^\varepsilon$ and ϱ_E^ε are the applied surface-forces and the surface electric charge, respectively. Obviously, for these conditions $\boldsymbol{u}^\varepsilon$ is determined up to a rigid body motion from the space $\mathrm{RBM}(\Omega_m^\varepsilon)$, and φ^ε up to a constant, provided solvability conditions are satisfied.

To obtain the effective material coefficients describing the piezo-poroelastic material in the limit for $\varepsilon \to 0$, the homogenization method is applied to the weak formulation of the problem (2)-(5) which reads, as follows: Find $(\boldsymbol{u}^\varepsilon, \varphi^\varepsilon, \bar{p}^\varepsilon) \in \mathbf{H}^1(\Omega_m^\varepsilon)/\mathrm{RBM}(\Omega_m^\varepsilon) \times H^1(\Omega_m^\varepsilon) \times \mathbb{R}$ such that:

$$\begin{aligned} &\int_{\Omega_m^\varepsilon} [\mathbb{A}^\varepsilon \boldsymbol{e}(\boldsymbol{u}^\varepsilon) - (\boldsymbol{g}^\varepsilon)^T \cdot \nabla\varphi^\varepsilon] : \boldsymbol{e}(\boldsymbol{v}) \,\mathrm{dV} + \bar{p}^\varepsilon \int_{\Gamma^\varepsilon} \boldsymbol{n}^{[m]} \cdot \boldsymbol{v} \,\mathrm{dS}_x = \int_{\partial_{\mathrm{ext}}\Omega_m^\varepsilon} \boldsymbol{h}^\varepsilon \cdot \boldsymbol{v} \,\mathrm{dS}_x + \int_{\Omega_m^\varepsilon} \boldsymbol{f}^\varepsilon \cdot \boldsymbol{v} \,\mathrm{dV} \,, \\ &\int_{\Omega_m^\varepsilon} [\boldsymbol{g}^\varepsilon : \boldsymbol{e}(\boldsymbol{u}^\varepsilon) + \boldsymbol{d}^\varepsilon \cdot \nabla\varphi^\varepsilon] \cdot \nabla\psi = \int_{\Omega_m^\varepsilon} q_E^\varepsilon \psi \,\mathrm{dV} + \int_{\partial_{\mathrm{ext}}\Omega_m^\varepsilon} \varrho_E^\varepsilon \psi \,\mathrm{dS}_x \,, \\ &\int_{\partial\Omega_c^\varepsilon} \widetilde{\boldsymbol{u}^\varepsilon} \cdot \boldsymbol{n}^{[c]} \,\mathrm{dS}_x + \gamma^\alpha \bar{p}^\varepsilon |\Omega_c^\varepsilon| = -J^\varepsilon \,, \end{aligned} \tag{6}$$

for all $(\boldsymbol{v}, \psi) \in \mathbf{H}^1(\Omega_m^\varepsilon) \times H^1(\Omega_m^\varepsilon)$.

2.2 Stokes flow through rigid porous structure

As pointed out above, the quasistatic viscous flow in the pores can be upscaled separately of the deformation problem. The steady flow problem through the channel network constituting domain Ω_c^ε is defined in terms of the flow velocity $\boldsymbol{w}^\varepsilon$ and pressure p^ε which satisfy the following equations:

$$\begin{aligned} -\eta^\varepsilon \nabla^2 \boldsymbol{w}^\varepsilon + \nabla p^\varepsilon &= \boldsymbol{f}^\varepsilon \,, \quad \text{in } \Omega_c^\varepsilon \,, \\ \nabla \cdot \boldsymbol{w}^\varepsilon &= 0 \,, \quad \text{in } \Omega_c^\varepsilon \,, \\ \boldsymbol{w}^\varepsilon &= 0 \,, \quad \text{on } \Gamma^\varepsilon \,, \\ -p^\varepsilon \boldsymbol{n}^{[c]} + \eta^\varepsilon \boldsymbol{n}^{[c]} \cdot \nabla \boldsymbol{w}^\varepsilon &= \boldsymbol{g}^\varepsilon \,, \quad \text{on } \partial_{\mathrm{ext}}\Omega_c^\varepsilon \,, \end{aligned} \tag{7}$$

where $\boldsymbol{g}^\varepsilon$ is given on the exterior boundary of the channels. It is worth to remark that $\boldsymbol{w}^\varepsilon$ describes the relative velocity of the fluid w.r.t. the solid phase.

By virtue of the small viscosity ansatz [1] we define $\eta^\varepsilon = \varepsilon^2\bar{\eta}$ which decreases with the scale. As discussed *e.g.* in [2], this viscosity scaling applies when the pores are small, so that an internal length scale characterizing the velocity profile in the pores is preserved in the limit $\varepsilon \to 0$.

3 The homogenized poroelastic model

The homogenization methods based on the two scale convergence or the unfolding operator techniques can be applied to describe the limit models arising from asymptotic analyses of the problems (6) and (7) for $\varepsilon \to 0$, cf. [8]. A consistent result has been obtained e.g. in [5].

In this short paper, we merely present the local problems for the so-called characteristic responses describing local fluctuations of the involved fields; the detail derivation of the upscaled model will be published in a forthcoming paper.

3.1 Local problems

We shall use the following bilinear forms:

$$\begin{aligned} a_Y^m(\boldsymbol{u},\,\boldsymbol{v}) &= |Y|^{-1}\int_{Y_m}[\mathbb{A}\boldsymbol{e}_y(\boldsymbol{u})] : \boldsymbol{e}_y(\boldsymbol{v})\;, \\ g_Y^m(\boldsymbol{u},\,\psi) &= |Y|^{-1}\int_{Y_m} g_{kij}e_{ij}^y(\boldsymbol{u})\partial_k^y\psi\;, \\ d_Y^m(\varphi,\,\psi) &= |Y|^{-1}\int_{Y_m}[\boldsymbol{d}\nabla_y\varphi]\cdot\nabla_y\psi\;. \end{aligned} \tag{8}$$

By $\fint_D = |Y|^{-1}\int_D$ with $D \subset \overline{Y}$ we denote the local average. We employ $\boldsymbol{\Pi}^{ij} = (\Pi_k^{ij})$, $i,j,k = 1,2,3$ with components $\Pi_k^{ij} = y_j\delta_{ik}$.

The local microstructural response is obtained by solving the following decoupled problems for the characteristic responses $(\boldsymbol{\omega},\vartheta)$ associated with the macroscopic variables: strain, electric field and the pore pressure.

- Find the strain correctors $(\boldsymbol{\omega}^{ij},\vartheta^{ij}) \in \mathbf{H}^1_\#(Y_m)\times H^1_\#(Y_m)$ for any $i,j = 1,2,3$ satisfying

$$\begin{aligned} a_Y^m\left(\boldsymbol{\omega}^{ij}+\boldsymbol{\Pi}^{ij},\,\boldsymbol{v}\right) - g_Y^m\left(\boldsymbol{v},\,\vartheta^{ij}\right) &= 0\;, \quad \forall\boldsymbol{v}\in\mathbf{H}^1_\#(Y_m)\;, \\ g_Y^m\left(\boldsymbol{\omega}^{ij}+\boldsymbol{\Pi}^{ij},\,\psi\right) + d_Y^m\left(\vartheta^{ij},\,\psi\right) &= 0\;, \quad \forall\psi\in H^1_\#(Y_m)\;, \end{aligned} \tag{9}$$

- Find the electric field correctors $(\boldsymbol{\omega}^k,\vartheta^k) \in \mathbf{H}^1_\#(Y_m)\times H^1_\#(Y_m)$ for any $k = 1,2,3$ satisfying

$$\begin{aligned} a_Y^m\left(\boldsymbol{\omega}^k,\,\boldsymbol{v}\right) - g_Y^m\left(\boldsymbol{v},\,\vartheta^k+y_k\right) &= 0\;, \quad \forall\boldsymbol{v}\in\mathbf{H}^1_\#(Y_m)\;, \\ g_Y^m\left(\boldsymbol{\omega}^k,\,\psi\right) + d_Y^m\left(\vartheta^k+y_k,\,\psi\right) &= 0\;, \quad \forall\psi\in H^1_\#(Y_m)\;, \end{aligned} \tag{10}$$

- Find pore fluid pressure correctors $(\boldsymbol{\omega}^P, \vartheta^P) \in \mathbf{H}^1_{\#}(Y_m) \times H^1_{\#}(Y_m)$ satisfying

$$\begin{aligned} a_Y^m\left(\boldsymbol{\omega}^P,\, \boldsymbol{v}\right) - g_Y^m\left(\boldsymbol{v},\, \vartheta^P\right) &= \fint_{\Gamma_Y} \boldsymbol{v}\cdot\boldsymbol{n}^{[m]}\,\mathrm{dS}_y\;, \quad \forall \boldsymbol{v}\in\mathbf{H}^1_{\#}(Y_m)\;,\\ g_Y^m\left(\boldsymbol{\omega}^P,\, \psi\right) + d_Y^m\left(\vartheta^P,\, \psi\right) &= 0\;, \quad \forall \psi\in H^1_{\#}(Y_m)\;, \end{aligned} \tag{11}$$

3.2 Macroscopic model of the static piezo-poroelastic medium

Using the characteristic responses (9)–(11) obtained at the microscopic scale, the homogenized coefficients describing the effective properties of the deformable porous medium are given by the following expressions:

$$\begin{aligned} A^H_{klij} &= a_Y^m\left(\boldsymbol{\omega}^{ij}+\boldsymbol{\Pi}^{ij},\, \boldsymbol{\omega}^{kl}+\boldsymbol{\Pi}^{kl}\right) + d_Y^m\left(\vartheta^{kl},\, \vartheta^{ij}\right)\;,\\ B^H_{ij} &= a_Y^m\left(\boldsymbol{\omega}^P,\, \boldsymbol{\Pi}^{ij}\right) - g_Y^m\left(\boldsymbol{\Pi}^{ij},\, \vartheta^P\right) = -\fint_{Y_m} \mathrm{div}_y\boldsymbol{\omega}^{ij}\;,\\ M^H &= a_Y^m\left(\boldsymbol{\omega}^P,\, \boldsymbol{\omega}^P\right) + d_Y^m\left(\vartheta^P,\, \vartheta^P\right)\;,\\ D^H_{kl} &= d_Y^m\left(\vartheta^l + y_l,\, \vartheta^k + y_k\right) + a_Y^m\left(\boldsymbol{\omega}^k,\, \boldsymbol{\omega}^l\right)\;,\\ G^H_{kij} &= g_Y^m\left(\boldsymbol{\Pi}^{ij},\, \vartheta^k + y_k\right) - a_Y^m\left(\boldsymbol{\omega}^k,\, \boldsymbol{\Pi}^{ij}\right) = g_Y^m\left(\boldsymbol{\omega}^{kl}+\boldsymbol{\Pi}^{kl},\, y_k\right) + d_Y^m\left(\vartheta^{ij},\, y_k\right)\;,\\ F_i &= \fint_{\Gamma_Y} \boldsymbol{\omega}^i\cdot\boldsymbol{n}^{[m]}\,\mathrm{dS}_y = g_Y^m\left(\boldsymbol{\omega}^P,\, y_i\right) + d_Y^m\left(\vartheta^P,\, y_i\right)\;. \end{aligned} \tag{12}$$

Further we define:

$$\hat{B}_{ij} = B^H_{ij} + \phi\delta_{ij}\;, \qquad \hat{M} = M^H + \gamma\phi\;. \tag{13}$$

The macroscopic problem reads, as follows: Find $(\boldsymbol{u}^0, \varphi^0) \in \mathbf{H}^1(\Omega)/\mathrm{RBM}(\Omega)\times H^1(\Omega)/\mathbb{R}$ and $\bar{p}\in\mathbb{R}$, such that

$$\begin{aligned} &\int_\Omega [\mathbb{A}^H\boldsymbol{e}(\boldsymbol{u}^0) - (\underline{\boldsymbol{G}}^H)^T\nabla\varphi^0 - \bar{p}\hat{\boldsymbol{B}}] : \boldsymbol{e}(\boldsymbol{v}^0)\,\mathrm{dV} = \int_\Omega \hat{\boldsymbol{f}}\cdot\boldsymbol{v}^0\;\mathrm{dV} + \int_{\partial\Omega}\overline{\boldsymbol{h}}(\bar{p})\cdot\boldsymbol{v}^0\,\mathrm{dS}_x\;,\\ &\int_\Omega [\underline{\boldsymbol{G}}^H\boldsymbol{e}(\boldsymbol{u}^0) + \boldsymbol{D}^H\nabla\varphi^0 - \underline{F}\bar{p}]\cdot\nabla\psi^0\,\mathrm{dV} = \int_\Omega \hat{q}_E\psi^0\,\mathrm{dV} + \int_{\partial\Omega}\overline{\varrho_E}\psi^0\,\mathrm{dS}_x\;,\\ &\int_\Omega \left(\hat{\boldsymbol{B}} : \boldsymbol{e}(\boldsymbol{u}^0) - \underline{F}\cdot\nabla\varphi^0 + \hat{M}\bar{p}\right)\,\mathrm{dV} = -J\;, \end{aligned} \tag{14}$$

for all $(\boldsymbol{v}^0, \psi^0) \in \mathbf{H}^1(\Omega)\times H^1(\Omega)$.

To conclude this section, we write the effective constitutive equations for the upscaled porous piezoelectric material:

$$\begin{aligned} \boldsymbol{\sigma}^H &= \mathbb{A}^H\boldsymbol{e}(\boldsymbol{u}) - (\underline{\boldsymbol{G}}^H)^T\nabla\varphi - p\hat{\boldsymbol{B}}\;,\\ \vec{D} &= \underline{\boldsymbol{G}}^H\boldsymbol{e}(\boldsymbol{u}) + \boldsymbol{D}^H\nabla\varphi - \underline{F}p\;,\\ -p &= \frac{1}{\hat{M}}\left(\hat{\boldsymbol{B}} : \boldsymbol{e}(\boldsymbol{u}) - \underline{F}\cdot\nabla\varphi + j\right)\;, \end{aligned} \tag{15}$$

where j is the local fluid volume production in the porous material; in fact $j = \nabla\cdot\boldsymbol{w}$, where $\boldsymbol{w}$ is the seepage velocity. As the consequence of (15), the pressure can be eliminated from $(15)_{1,2}$, so that

$$\begin{aligned} \boldsymbol{\sigma}^H &= \hat{\mathbb{A}}^H \boldsymbol{e}(\boldsymbol{u}) - (\hat{\underline{\boldsymbol{G}}}^H)^T \nabla\varphi + \hat{M}^{-1}\hat{\boldsymbol{B}} j \ , \\ \vec{D} &= \hat{\underline{\boldsymbol{G}}}^H \boldsymbol{e}(\boldsymbol{u}) + \hat{\boldsymbol{D}}^H \nabla\varphi + \hat{M}^{-1}\underline{F} j \ , \end{aligned} \tag{16}$$

where

$$\begin{aligned} \hat{\mathbb{A}}^H &= \mathbb{A}^H + \hat{M}^{-1}\hat{\boldsymbol{B}}\otimes\hat{\boldsymbol{B}} \quad \text{undrained elasticity} \ , \\ \hat{\boldsymbol{D}}^H &= \boldsymbol{D}^H - \hat{M}^{-1}\underline{F}\otimes\underline{F} \quad \text{undrained dielectricity} \ , \\ \hat{\underline{\boldsymbol{G}}}^H &= \underline{\boldsymbol{G}}^H + \hat{M}^{-1}\underline{F}\hat{\boldsymbol{B}} \quad \text{undrained piezoelectric coupling} \ . \end{aligned} \tag{17}$$

The upscaled piezoelectric effect incorporates the electric field induced by increasing the fluid pressure, or fluid contents in the pores. Let us consider injection of a fluid under the pressure $\bar{p}$ into the porous structure such that the macroscopic deformation is disabled. If $\vec{D} = \vec{0}$ (insulated boundary and no volume charge), then the following electric field is established (the fluid content increased by j, see (16))

$$\nabla\varphi = (\boldsymbol{D}^H)^{-1}\underline{F}\bar{p} \ , \ \text{or} \ \nabla\varphi = -(\hat{M}\hat{\boldsymbol{D}}^H)^{-1}\underline{F} j \ . \tag{18}$$

4 Flow in the homogenized fluid-saturated piezo-poroelastic medium

As mentioned earlier, if the inertia effects are neglected, the upscaling result can be obtained in two independent steps. From (14), we obtain the mathematical model describing the static response of the medium, thus no flow occurs. Then, the effective flow of an electrically neutral fluid in the porous material governed by the Darcy law involving the intrinsic hydraulic permeability $\boldsymbol{K}^H$ and the fluid viscosity $\bar{\eta}$. In (14), the last equality can be interpreted locally. Let $p(t,x)$ be the local pressure and $\boldsymbol{w}(t,x)$ the effective flow seepage velocity describing the relative effective fluid velocity w.r.t. the solid skeleton, *i.e.* $\boldsymbol{w} = \phi(\boldsymbol{v}^f - \dot{\boldsymbol{u}})$, where $\boldsymbol{v}^f$ is the mean fluid velocity. Then from $(14)_3$, dropping the superscripts ^{0}, we can derive the following equation:

$$\hat{\boldsymbol{B}} : \boldsymbol{e}(\dot{\boldsymbol{u}}) - \underline{F}\cdot\nabla\dot{\varphi} + \hat{M}\dot{p} + \nabla\cdot\boldsymbol{w} = 0 \ , \ \text{where} \quad \boldsymbol{w} = -\bar{\eta}^{-1}\boldsymbol{K}^H\nabla p \ . \tag{19}$$

The Darcy flow model is the classical result, obtained upon homogenizing the Stokes problem (7), see *e.g.* [1, 2].

Below we present the problem describing the viscous flow in the piezo-poroelastic medium characterized by the effective model parameters (12) and (13). To introduce boundary conditions for the coupled problem, we need the following 3 decompositions of $\partial\Omega$ into disjoint parts:

$$\begin{aligned} \partial\Omega &= \partial_\sigma\Omega \cup \partial_u\Omega \ , \quad \partial_\sigma\Omega \cap \partial_u\Omega = \emptyset \ , \\ \partial\Omega &= \partial_w\Omega \cup \partial_p\Omega \ , \quad \partial_w\Omega \cap \partial_p\Omega = \emptyset \ , \\ \partial\Omega &= \partial_E\Omega \cup \partial_\varphi\Omega \ , \quad \partial_E\Omega \cap \partial_\varphi\Omega = \emptyset \ . \end{aligned} \tag{20}$$

For the displacement, the electric potential and the pressure we may consider the following boundary conditions, where p_∂, w_n and $\boldsymbol{g}^s$ are given:

$$\begin{aligned} \boldsymbol{u} = \boldsymbol{0}\ , \quad & \text{on } \partial_u\Omega\ , \qquad \boldsymbol{n}\cdot\boldsymbol{\sigma} = \boldsymbol{g}^s\ , \quad \text{on } \partial_\sigma\Omega\ , \\ p = p_\partial\ , \quad & \text{on } \partial_p\Omega\ , \qquad \boldsymbol{n}\cdot\boldsymbol{w} = w_n\ , \quad \text{on } \partial_w\Omega\ , \\ \varphi = 0\ , \quad & \text{on } \partial_\varphi\Omega\ , \qquad \boldsymbol{n}\cdot\vec{D} = D_n\ , \quad \text{on } \partial_E\Omega\ . \end{aligned} \tag{21}$$

Therefore, the following spaces and admissibility sets are involved in the weak formulation:

$$\begin{aligned} \boldsymbol{U}(\Omega) &= \{\boldsymbol{u}\in\mathbf{H}^1(\Omega)|\ \boldsymbol{u}=\boldsymbol{0} \text{ on } \partial_u\Omega\}\ , \\ P(\Omega) &= \{p\in H^1(\Omega)|\ p=p_\partial \text{ on } \partial_p\Omega\}\ , \\ \Phi(\Omega) &= \{\varphi\in H^1(\Omega)|\ \varphi=0 \text{ on } \partial_\varphi\Omega\}\ . \end{aligned} \tag{22}$$

The space of test pressure functions $P_0(\Omega)$ is defined according to $(22)_2$ with $p_\partial \equiv 0$ while test displacements belong to $\boldsymbol{U}_0(\Omega)$ which is identified with $\boldsymbol{U}(\Omega)$ due to (21). In analogy, $\Phi_0(\Omega) = \Phi(\Omega)$ is considered as the space of the test electric potentials.

We are now in a position to introduce the weak formulation of the macroscopic problem for the piezo-poroelastic medium. The zero initial conditions are considered for simplicity, i.e. $\boldsymbol{u}(\cdot, t=0) = 0$, $p(\cdot, t=0) = 0$, and $\varphi(\cdot, t=0) = 0$. For any time $t > 0$, the following system is to be satisfied by $(\boldsymbol{u}, \varphi, p) \in \boldsymbol{U}(\Omega)\times\Phi(\Omega)\times P(\Omega)$

$$\begin{aligned} &\int_\Omega [\mathbb{A}^H\boldsymbol{e}(\boldsymbol{u}) - (\underline{\boldsymbol{G}}^H)^T\nabla\varphi - p\hat{\boldsymbol{B}}] : \boldsymbol{e}(\boldsymbol{v})\,\mathrm{dV} = \int_\Omega \hat{\boldsymbol{f}}\cdot\boldsymbol{v}\ \mathrm{dV} + \int_{\partial_\sigma\Omega}\boldsymbol{g}^s\cdot\boldsymbol{v}\,\mathrm{dS}_x\ , \\ &\int_\Omega [\underline{\boldsymbol{G}}^H\boldsymbol{e}(\boldsymbol{u}) + \boldsymbol{D}^H\nabla\varphi - \underline{F}p]\cdot\nabla\psi\,\mathrm{dV} = \int_\Omega \hat{q}_E\psi\,\mathrm{dV} + \int_{\partial_E\Omega} D_n\psi\,\mathrm{dS}_x\ , \\ &\int_\Omega \zeta\left(\hat{\boldsymbol{B}} : \boldsymbol{e}(\dot{\boldsymbol{u}}) - \underline{F}\cdot\nabla\dot{\varphi} + \hat{M}\dot{p}\right)\ \mathrm{dV} + \int_\Omega \nabla\zeta\cdot\bar{\eta}^{-1}\boldsymbol{K}^H(\nabla p - \boldsymbol{f}^f)\ \mathrm{dV} = \int_{\partial_w\Omega} w_n\zeta\,\mathrm{dS}_x\ , \end{aligned} \tag{23}$$

for all $(\boldsymbol{v}, \psi, \zeta) \in \boldsymbol{U}_0(\Omega)\times\Phi_0(\Omega)\times P_0(\Omega)$.

5 NUMERICAL EXAMPLES

We shall illustrate features of the homogenized piezo-poroelastic material using a numerical simulation of a compaction test. To compute numerical solutions of the local problems (9)-(11) at the micro-level and those of the macroscopic problem (23), we use the standard FE method using piecewise linear (conforming) approximation for the macroscopic fields $\boldsymbol{u}$, p, and φ, and the corrector fields $(\boldsymbol{\omega}, \vartheta)$. The macroscopic specimen with dimensions $2h\times 2h\times h$, with $h = 1$ cm, and the representative periodic cell Y generating the porous structure are depicted in Fig. 2. In Tab. 1, the homogenized coefficients are compared with those of the piezoelectric material $BaTiO_3$ constituting the skeleton Y_m. The other homogenized coefficients of the upscaled porous medium are listed in Tab. 2.

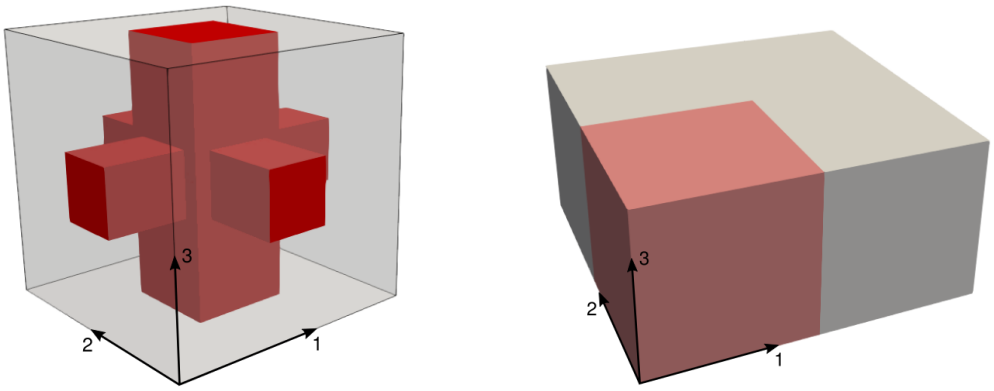

Figure 2: Left: periodic cell Y representing piezoelectric porous microstructure; gray part: solid matrix, red part: fluid channel. Right: Macroscopic domain Ω, only one quarter (as emphasized by the red colour) is used to solve the macroscopic problem due to its symmetry.

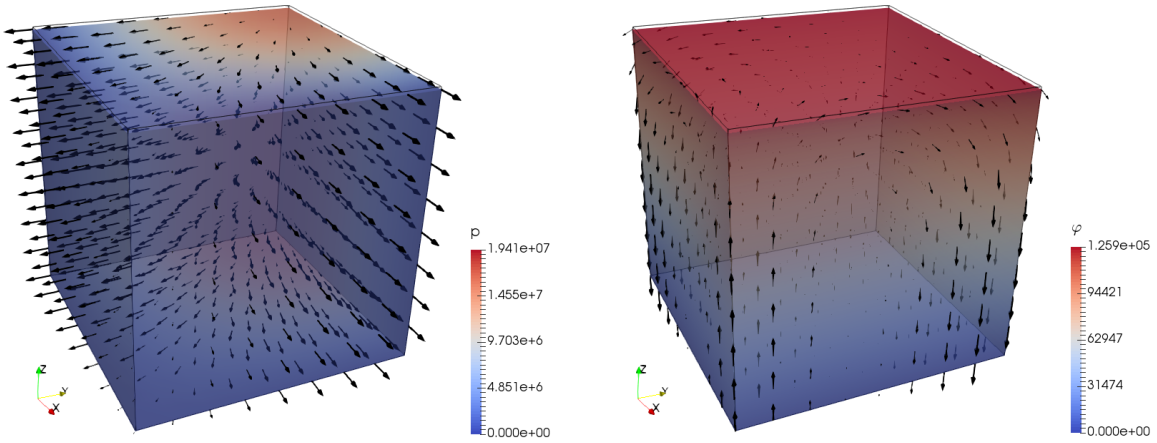

Figure 3: Deformed state of the drained macroscopic specimen at time $t = 0.8\,\mathrm{ms}$ Left: macroscopic pressure p and seepage velocity $\boldsymbol{w}$ (depicted by arrows, max. magnitude $= 7.126 \cdot 10^{-3}$ m/s); Right: electric potential φ and electric displacement $\vec{D}$ (depicted by arrows, max. magnitude $= 3.016 \cdot 10^{-5}$ C/m^2).

elasticity: (in 10× GPa)	A_{1111}	A_{3333}	A_{1122}	A_{2233}	A_{1313}	A_{1212}
skeleton:	15.040	14.550	6.560	6.590	4.240	4.390
homog. porous:	7.816	8.614	2.343	2.724	2.419	1.838

piezo-coupling: (in C/m^2)	G_{311}	G_{322}	G_{333}	G_{223}
skeleton:	-4.322	-4.322	17.360	11.404
homog. porous:	-1.483	-1.483	12.663	6.046

dielectricity: (in 10^{-9} C/Vm)	D_{11}	D_{33}
skeleton:	8.456	10.651
homog. porous:	1.284	1.505

Table 1: Piezoelectric properties of the skeleton and of the homogenized porous material. The transverse isotropy yields the following symmetries: $A_{2233} = A_{1133}$, $A_{1313} = A_{2323}$, $G_{311} = G_{322}$, $G_{223} = G_{113}$, $D_{11} = D_{22}$. Other components are zero.

$\hat{B}_{11}$	$\hat{B}_{33}$	$\hat{M}$	F_3	K_{11}	K_{33}
-	-	10^{-2}/GPa	10^{-11}×m/V	$^{-11}\times$ m^2	$^{-11}\times$ m^2
0.548	0.464	5.352	-1.274	2.474	7.741

Table 2: Homogenized coefficients. Note the symmetries $\hat{B}_{11} = \hat{B}_{22}$, $K_{11} = K_{22}$, other components are zero. Note that the physical permeability is ε_0^2 times smaller, thus, $K_{11}/\bar{\eta} = 2.604 \times 10^{-12}$ m / Pa·s.

Although the homogenized coefficients computed using (12) and (13) are independent of the microstructure size, the hydraulic permeability depends on $\varepsilon_0 > 0$ by virtue of the permeability scaling; we used $\varepsilon_0 = 10^{-4}$, thus the microstructure size is $\ell = 0.1$ mm. Therefore, $\bar{\eta} = \eta/\varepsilon_0^2 = 0.950 \times 10^{-8}$ Pa·s for glycerin considered as the pore fluid with its compressibility $\gamma = 2.30 \times 10^{-10}\,\mathrm{Pa}^{-1}$.

We considered the drained (case I) and undrained (case II) compaction of the macroscopic specimen. In both the cases, the following conditions were prescribed; bottom side: $\boldsymbol{u} \cdot \boldsymbol{n} = 0$, $w_n = 0$, $\varphi = 0$, top side: prescribed $\bar{u} = \boldsymbol{u} \cdot \boldsymbol{n} = -10^{-3} s(t)$ m, $w_n = 0$, $D_n = 0$. The loading function $s(t)$ describes the ramp-and-hold test (the plato for $t > 0.5$ ms). On lateral faces of the specimen, $p = 0$ in case I (drained), while $w_n = 0$ in case II (undrained). No volume forces are considered, thus, $\boldsymbol{f}^f = \hat{\boldsymbol{f}} = \boldsymbol{0}$ in (23).

For case I, in Fig. 3 the pressure, the seepage velocity, and the electric fields are depicted for the deformed state at $t = 0.8$ ms. The spatial pressure variation leads to a nonvanishing field $\vec{D}(x)$; obviously, $\vec{D}$ vanishes in the case II due to the homogeneous distribution of $\boldsymbol{e}(\boldsymbol{u})$, p and $\nabla\varphi$. In Fig. 4 time variation $p(x^A, t)$, $\varphi(x^A, t)$, and $e_{23}(x^A, t)$ is displayed at a point A situated in the middle of the computational domain, $x^A = [0.5h, 0.5h, 0.5h]$ cm, see Fig. 2. While all quantities are constant for the case II in the plato, $t > 0.5$ ms, they change in the case I.

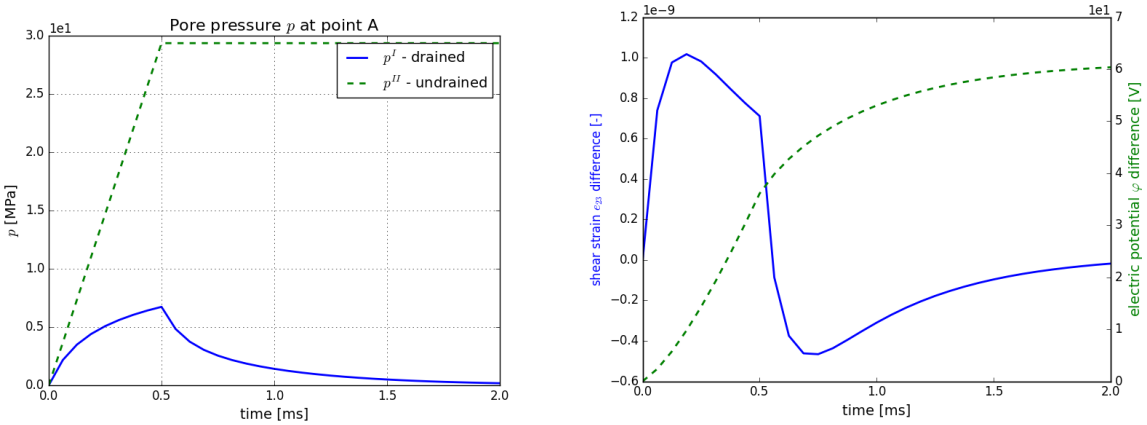

Figure 4: Left: Comparison of time evolution of pressures p^I, p^{II} at macroscopic point A. Right: Difference of the strain component $e^{II}_{23} - e^I_{23}$ (blue solid line) and of the electric potential $\varphi^{II} - \varphi^I$ (green dashed line) at macroscopic point A.

6 CONCLUSIONS

In the present paper we studied the piezoelectric properties of the periodic porous media saturated by viscous fluids under quasistatic loadings. Using the periodic homogenization method, the effective medium coefficients were derived. The porous materials enable to generate the electric field without any macroscopic deformation, just due to an injected volume of fluid in the pores. In the upscaled model, this is respected by the new vector coefficient $\underline{F}$ which is associated with the polarization of the piezomatrial constituting the skeleton. We have shown, how the piezoelectric properties influence the Biot stress coupling coefficients and the Biot compressibility. It is worth noting that the model describes flow of a neutral fluid, whereby electric insulation was considered on the pore surface.

Although the derived model describes the linear response of the homogenized medium, it can be adapted to capture some nonlinear effects, namely those associated with the fluid flow in the pores. Assuming the linear kinematics framework, in [6], we proposed a weakly nonlinear model of the Biot continuum, where the nonlinearity in the homogenized continuum is introduced in terms of the deformation-dependent material coefficients which are approximated as linear functions of the macroscopic response. These functions are obtained by the sensitivity analysis of the homogenized coefficients computed for a given geometry of the porous structure which transforms due to the local deformation. The deformation-dependent material coefficients approximated in this way do not require any solving of local microscopic problems for updated configurations. To deal with the piezo-poroelastic material, we adhere the same approach of [6] and employ the sensitivity analysis developed for the piezoelectric composites in [7].

Acknowledgment This research is supported by project GACR 16-03823S and in part by project LO 1506 of the Czech Ministry of Education, Youth and Sports.

REFERENCES

[1] Hornung, U. *Homogenization and porous media*, Interdisciplinary Applied Mathematics, Springer, Vol. 6 (1997).

[2] Iliev, O., Mikelic, A. and Popov, P. On upscaling certain flows in deformable porous media. *SIAM, Multiscale Model. Simul.* (2008) **7**:93–123.

[3] Iyer, S. and Venkatesh, T.A. Electromechanical response of (3-0, 3-1) particulate, fibrous, and porous piezoelectric composites with anisotropic constituents: A model based on the homogenization method. *International Journal of Solids and Structures* (2014) **51**:1221–1234.

[4] Miara, B., Rohan, E., Zidi, M. and Labat, B. Piezomaterials for bone regeneration design - homogenization approach. *Jour. of the Mech. and Phys. of Solids* (2005) **53**:2529–2556.

[5] Mikelic, A. and Wheeler, M. On the interface law between a deformable porous medium containing a viscous fluid and an elastic body. *Math. Models Meth. Appl. Sci.* (2012) **22**:1–32.

[6] Rohan, E. and Lukeš, V. On modelling nonlinear phenomena in deforming heterogeneous media using homogenization and sensitivity analysis concepts. *Applied Mathematics and Computation* (2015) **267**:583–595.

[7] Rohan, E. and Miara, B. Homogenization and shape sensitivity of microstructures for design of piezoelectric bio-materials. *Mechanics of Advanced Materials and Structures* (2006) **13**:473–485.

[8] Rohan, E., Naili, S. and Lemaire, T. Double porosity in fluid-saturated elastic media: deriving effective parameters by hierarchical homogenization of static problem. *Continuum Mech. Thermodyn.* (2016) **28**:1263–1293.

[9] Koutsawa, Y., Belouettar, S., Makradi, A. and Nasser, H. Sensitivities of effective properties computed using micromechanics differential schemes and high-order Taylor series: Application to piezo-polymer composites. *Mechanics Research Communications* (2010) **37**:489–494.

[10] Vashishth, A.K., and Gupta, V. Wave propagation in transversely isotropic porous piezoelectric materials *International Journal of Solids and Structures* (2009) **46**:3620–3632.